Modeling and Optimization of CMOS Compatible Various ZnO/SiO₂/Si Multilayer Structure for SAW Devices Using FEM

P.R. Bagade[1,*], A.J. Pawar[2], R.K. Kamat[2], S.A. Shinde[2,†]

[1] *Department of Electronics, Vivekanand College, (Autonomous) Kolhapur, Maharashtra, India*
[2] *Department of Electronic, Shivaji University, Kolhapur, Maharashtra, India*

This article presents a design, modeling and optimization of Surface Acoustic Wave (SAW) resonator with CMOS compatible piezoelectric crystal material and characterized for wireless 915 MHz ISM frequency band. Simulation study for the realization of SAW resonator based on CMOS compatible piezoelectric thin film of Zinc oxide (ZnO) on passivated silicon (SiO₂/Si) substrate is performed. The SAW properties of ZnO film on SiO₂/Si were analyzed with three composite structures as (IDT)/ZnO/SiO₂/Si, ZnO/(IDT)/ZnO/SiO₂/Si, and ZnO/(IDT)/SiO₂/Si using COMSOL Multiphysics Software. The properties of ZnO/(IDT)/SiO₂/Si structure revealed good SAW properties such as maximum coupling coefficient and acoustic velocity compared to other structures. The effects of piezoelectric Zinc oxide (ZnO) layer, interdigital transducer (IDT) materials, and SiO₂ thin film thickness on the evolution of the phase velocity and electromechanical coupling coefficient (K^2) were studied by employing a finite element method. The design and simulations of multilayered SAW structure carried out for 915 MHz and ZnO/(IDT)/SiO₂/Si structure provide excellent overall performance.

Keywords: SAW device, Finite element method (FEM), MEMs, Interdigital transducer (IDT).

1. INTRODUCTION

SAW devices offers several advantages such as low power consumption, high frequency operation, high stability and reliability and hence now widely used in various applications viz. mobile communication, electronics industries, microfluidic, and various biological and environment sensor. As the novel telecom operating at higher frequency band with larger bandwidth need the devices operating at GHz range SAW devices are the ultimate solution for all such high frequency applications. SAW devices and film bulk acoustic resonators has become an emerging research hotspot to develop a filter, duplexer, and resonator with a new features and tougher specifications for current and future front-end RF modules. SAW devices with a large SAW velocity, larger electromechanical coupling coefficient (K2), higher quality factor(Q), and smaller temperature coefficient of frequency (TCF) will meet the existing 4G communication system equipment and future developing 5G mobile communication system. Hence, it is requirement to design and develop advanced SAW devices to support a next-generation communication system [1-2]. Surface Acoustic Wave (SAW) consists of three main parts as substrate material, piezoelectric thin layer, and Interdigital transducers (IDTs). An IDTs structure consists of a comb-shaped periodic metallic structure on a piezoelectric substrate, which converts electric energy signal into acoustic wave signal and vice versa. The pitch of the IDT pattern determines the operating frequency of the device. Piezoelectric layer plays an important role in the design and performance of devices corresponding to size, acoustic velocity, and CMOS compatibility [3]. Thus, the performance of the SAW device depends on the IDT pattern and piezoelectric substrate material. Recently, fabrication of pitch of the IDTs pattern for a maximum frequency of operation is limited by the photolithography resolution. Hence, varying the piezoelectric substrate materials with high acoustic velocity is the key to achieve high-frequency SAW devices [4].

Traditionally, SAW devices are fabricated over the piezoelectric bulk substrate, such as Lithium tantalite (LiTaO₃), Lithium-niobate (LiNbO₃), and Quartz. These bulk substrate configurations were brittle, had low acoustic velocity, and were not feasible to integrate with microelectronic circuitry. As a result, the realization of integrated CMOS compatibility and high-frequency saw devices with bulk substrate become challenging [5]. To fulfill the current requirement of corresponding to high phase velocity, device miniaturization, temperature compensation, and compatibility to CMOS technology, layered piezoelectric thin film structure of saw devices have been investigated. Because of these unique advantages of multilayered structure, several research works have been published on investigated the propagation characteristic of SAW device in multilayer structure like ZnO/Si, ZnO/AIN/Si,AIN/Diamond/Si, and SiO₂/IDT/LiNbO₃/Diamond/Si [1]. Recently, piezoeletric thin films like zinc oxide (ZnO), aluminum nitride (AIN), and lead zirconate titanate (PZT) are commonly uses thin film materials for acoustic devices technology [6]. Assouar et al. has been reported that the preferred orientation of AlN thin films deposited on the diamond by reactive RF magnetron sputtering can achieve the SAW velocity approximately in the range 10.000 m/s to 12.000 m/s. This high acoustic velocity benefit allows developing the high-frequency SAW devices using e-beam lithography operating at frequencies up to 8 GHz on an AlN/diamond multilayer structure [7]. However, AIN displays low electromechanical coupling coefficient [8]. In general, ZnO exhibits good piezoelectric prop-

erties and is preferred for implementing SAW devices due to its high coupling coefficient. Along with that, it has high temperature stability and excellent bonding with various substrate materials, in particular silicon, so it is possible to fabricate low loss and small size SAW devices with CMOS compatible microfabrication technology [9]. It can be grown in thin film form by various deposition methods for microelectromechanical systems (MEMS) and other applications. These techniques are radio frequency (RF) sputtering [10], spray deposition [11], pulsed laser deposition technique [12], organic chemical vapor deposition method [13], and chemical bath deposition [14].Many researches have been studied and implemented SAW devices based on ZnO as a piezoelectric material thin film on different substrates for several applications. The feasibility of SAW filters in ZnO/SiO₂/Si layered structures and their silicon integrated monolithically CMOS circuitry in one single chip was reported by Visser et al. [15]. To improve the K2 and phase velocity of the SAW device, ZnO has been grown and proved on different materials such as IDT/ZnO/diamond [16], IDT/ZnO/SiO₂/Si[17], ZnO/XY-LiNbO₃ [18], and ZnO/SiO₂/Al₂O₃ [19] etc.

In this paper, we applied a two-dimensional finite element model (2D-FEM) to study SAW devices with CMOS compatible three different composite structures of ZnO/IDT/SiO₂/Si. The optimum design performance of the SAW resonator device for frequency 915 MHz was simulated using COMSOL Multiphysics software. An eigenfrequency analysis was conducted to find the device response. We obtain the SAW properties, including electromechanical coupling coefficient (K^2), phase velocity, and mechanical displacement properties of Rayleigh wave in three different composite ZnO/IDT/SiO₂/Si resonator structures. Also, we investigated the propagation characteristics of the SAW device by varying the thickness of the piezoelectric ZnO layer and the thickness of SiO₂ layer.

2. SAW DEVICE STRUCTURE AND SIMULATION METHODOLOGY

2.1 Device Structure

Surface acoustic waves (SAWs) are basically uses interdigital transducers patterned on a piezoelectric substrate to generate the electromechanical waves on the surface of a piezoelectric substrate. IDT's of SAW devices comprise periodic thin metal electrode comb-like structures. The acoustic waves are excited by the input IDT by applying an alternating voltage (AC) on a piezoelectric substrate, and subsequently, the received acoustic waves at the output port are reconverted into electric signals. The important parameter of designing the saw device is the center frequency (f_0), which is related to the wavelength (λ) and phase velocity (V_p) of SAW. It is calculated based on the following equation:

$$f_0 = \frac{V_p}{\lambda},$$

where λ is the wavelength, corresponds to the period IDT finger structure. With Rayleigh mode, the phase velocity for ZnO/SiO₂ structure is approximately 3600 m/s [20]. The IDT design and acoustic velocity of a substrate determines the resonant frequency (f_0) of the SAW device [21]. The SAW device with a multilayer structure creates

new development opportunities because of its unique combined properties such as high frequency of operation, high electromechanical coupling coefficient, improve stability, and low-temperature coefficients, which do not appear for bulk materials [22]. With multilayered structures, materials are combining with different properties in one stack can satisfy the requirements of low losses, size reduction, and high quality saw the device [23].

In this study, the three different configurations of ZnO/SiO2/Si layered structure are considered for study as (IDT)/ZnO/SiO2/Si, ZnO/(IDT)/ZnO/SiO2/Si, and ZnO/(IDT)/SiO2/Si. Fig. 1 gives the detailed schematic representation of the 2D single-cell multilayered SAW device model.The design parameter of the 915 MHz CMOS compatible saw resonator device is listed in the Table 1.

Table 1 – Design parameter of 915 MHz SAW resonator device

Parameters	Value
Wavelength(λ)	3.934 μm
Pitch of electrode ($\lambda/2$)	1.967 μm
Interdigital transducer (IDT) width	0.983 μm
Normalized ZnO thickness $t(ZnO)/\lambda$	0.1 to 0.8
IDT electrode height (0.05λ)	0.1967 μm
Thickness of SiO₂(t_{SiO2})	0.1 μm
Si substrate height (10 λ)	39.34 μm

2.2 Device Simulation by FEM

To achieve the objective of low cost and high-quality SAW device, it is necessary precise SAW device simulation with the suitable material and geometrical shapes of electrodes [24]. SAW propagation is described by differential equations that must be solved along with the geometric structure complexity of the device, the piezoelectric material properties and, the applied boundary conditions. FEM gives numerical solutions to associated differential equations that couples structure domain and electrical domain under constant stress and strain conditions [25]. COMSOL Multiphysics software used to perform 2D finite element method (FEM) analysis of piezoelectric layered SAW device. Finite Element Method (FEM) is used to describe the electromechanical coupling between the strain (S), stress (T), electric field (E), and electric displacement field (D) in a stress-charge of a piezoelectric crystal. This piezoelectric coupling phenomenon is governed by the piezoelectric constructive equations[1]given by:

$$D = [e][S] + [\varepsilon_S]E \qquad (1)$$

$$T = [c_E][S] - [e^t]E \qquad (2)$$

In the above, (1) and (2) is the piezoelectric constitute equation, D is electrical displacement density because of applied external electric field E, [ε_S] is dielectric permittivity, [S] is the material strain matrix, [e] is piezoelectric coefficient matrix, T is the mechanical stress produce by material strain, [c_E] is the elastic stiffness coefficient. The [e^t] matrix is the 3×6 transposed matrix of the piezoelectric constant matrix [1].
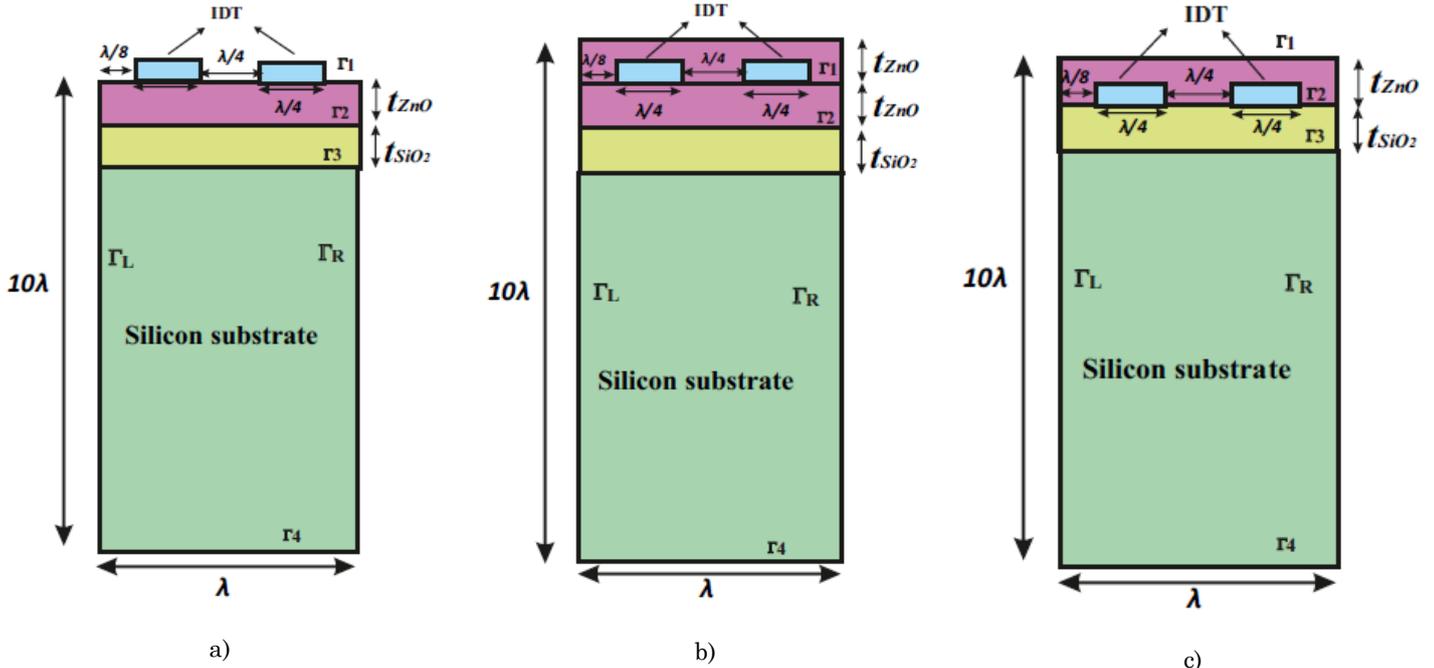
Fig. 1 – A 2D geometry of the periodic unit cell used in Finite Element Method (FEM) simulation for multilayered SAW structure as: a) (IDT)/ZnO/SiO₂/Si, b) ZnO/(IDT)/ZnO/SiO₂/Si, and c) ZnO/(IDT)/SiO₂/Si

Table 2 – Material Constant used in the simulations [15, 26]

	Symbol	ZnO	SiO$_2$	Si
Density(Kg/m^3)		5610	2200	2330
Elastic Constants(GPa)	C_{11}	1.57	78.5	166
	C_{12}	0.89	16.1	64
	C_{13}	0.83	16.1	64
	C_{33}	2.08	78.5	166
	C_{44}	0.38	31.2	80
	C_{66}	0.34	31.2	80
Piezoelectric Constant(C/m^2)	e_{15}	-0.59	–	–
	e_{31}	-0.61	–	–
	e_{33}	1.14	–	–
Dielectric Constant (10^{-11} F/m)	ε_{11}	3.3468	3.32	10.62
	ε_{33}	3.3468	3.32	10.62
Poisson ratio		–	0.33	0.17	0.27

In eigen mode, the acoustic wave velocity is Rayleigh modes calculated [21] by

$$V = f_0 x \lambda ,$$

Where f_0 is the resonance frequency obtained from simulation and λ is the wavelength of an acoustic wave.

The efficiency of the energy conversion between the electric signal and acoustic wave is estimated by the electromechanical coupling coefficient (K^2) parameter and is given with series and parallel resonance frequency [1] as

$$K^2 = \frac{\pi^2}{4} \frac{f_s - f_p}{f_s} ,$$

where *fs* and *fp* are series and parallel resonance frequency of SAW structure extracted from COMSOL Multiphysics simulation software.

3. RESULTS

In this section, we discuss the effect of the thickness variation of the ZnO thin film and thickness variation of the SiO₂ buffer layer on the performance of three multilayer CMOS compatible SAW structure. The performance of the proposed SAW device has been analyzed in terms of the electromechanical coupling coefficient (K^2) and phase velocity.

3.1 (IDT)/ZnO/SiO₂/Si Structure

(a)

(b)
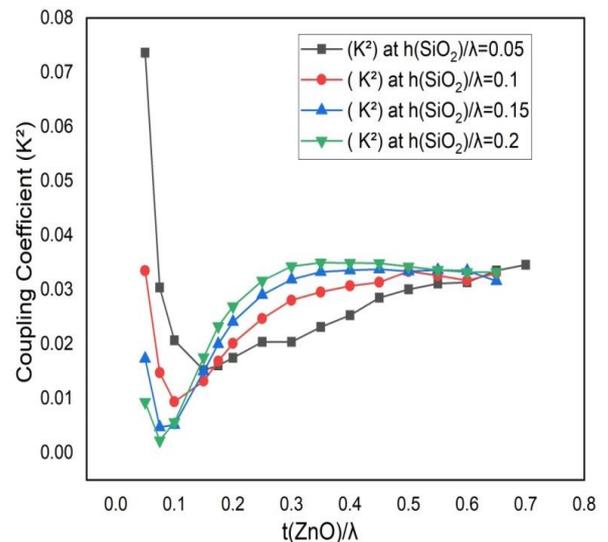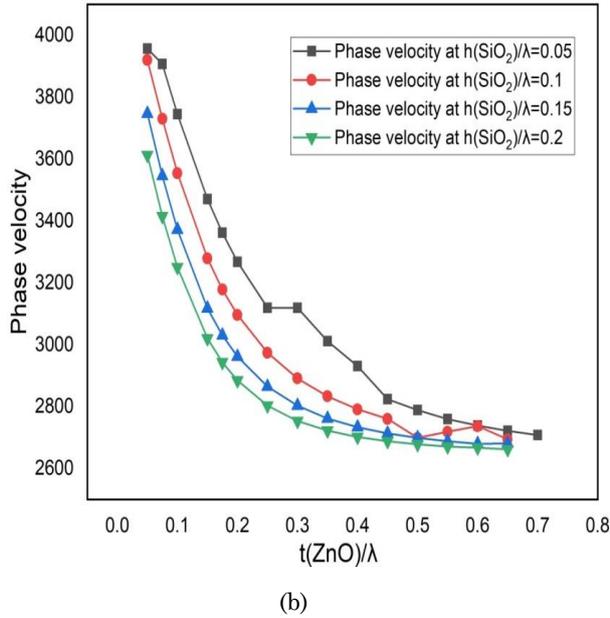
Fig. 2 – Simulated result of a) coupling coefficient (K2) b) phase velocity of Rayleigh mode generated in (IDT)/ZnO/SiO₂/Si structure as a function of the normalized thickness of ZnO for different normalized thicknesses of SiO₂

For (IDT)/ZnO/SiO₂/Si structure, the coupling coefficient start from 0.0736 and phase velocity 3900 m/s at the normalized thickness of $(t_{(ZnO)}/\lambda) = 0.05$ for normalized thicknesses of $(t_{(SiO2)}/\lambda) = 0.05$. The K^2 value reduces rapidly and reaches 0.016 at of $(t_{(ZnO)}/\lambda) = 0.175$ and increases slowly to 0.034 with increase in $(t_{(ZnO)}/\lambda)$ from 0.1 to 0.7. However, for normalized thickness of $(t_{(SiO2)}/\lambda) = 0.1, 0.15$, and 0.2, the value of K^2 is almost become constant for $(t_{(ZnO)}/\lambda)$ from 0.2 to 0.8. According to Fig. 2b, with the increase in the normalized thickness of ZnO from 0.05 to 0.3, the values of phase velocity are found to decrease rapidly and then saturate near the value of bulk ZnO. Also, it is clear that, the overall phase velocity nature showed a decreasing trend with increased normalized thicknesses of SiO₂.

3.2 ZnO/ (IDT)/ZnO/SiO₂/Si Structure

From the coupling coefficient curve shown in Fig. 3a, we found that K^2 increases suddenly from 0.0494 and reached the maximum value of 0.0949 with the increase in normalized thickness of $(t_{(ZnO)}/\lambda) = 0.05$ to 0.1 for the thicknesses of SiO₂ set to be $(t_{(SiO2)}/\lambda) = 0.2$. Further increase in thickness of $(t_{(ZnO)}/\lambda) = 0.1$ to 0.7, the K^2 value decreases linearly from its peak value. According to Fig. 3b, we observe the phase velocity of Rayleigh mode rapidly decreases from its peak value 3961 m/s to 2740 m/s with increasing normalized ZnO film thickness $(t_{(ZnO)}/\lambda) = 0.05$ to 0.3 at constant value $(t_{(SiO2)}/\lambda) = 0.05$. Further, with the increase of $(t_{(ZnO)}/\lambda) = 0.3$ to 0.7, the phase velocity shows a little change.

3.3 ZnO/(IDT)/SiO₂/Si Structure

The 2D-FEM simulation results for the SAW propagation characteristics in the ZnO/(IDT)/SiO₂/Si structure are presented in Fig. 4 (a, b). As shown in Fig. 4a,

the K^2 first increases with an increase in normalized thickness of ZnO, reaches the maximum value of 0.133 when $(t_{(ZnO)}/\lambda) = 0.1$ for the constant thicknesses value of SiO₂ to $(t_{(SiO2)}/\lambda) = 0.2$, and then the value of K^2 starts to decrease with a further increase in $(t_{(ZnO)}/\lambda)$. As displayed in Fig. 4b, the value of the phase velocity changes rapidly from 4385 m/s to 3026 m/s with the increase in the normalized thickness $(t_{(ZnO)}/\lambda)$ from 0.05 to 0.3. However, with the increase of the normalized ZnO layer thicknesses $(t_{(ZnO)}/\lambda)$ from 0.3 to 0.7, the phase velocity becomes almost constant.

(a)

(b)
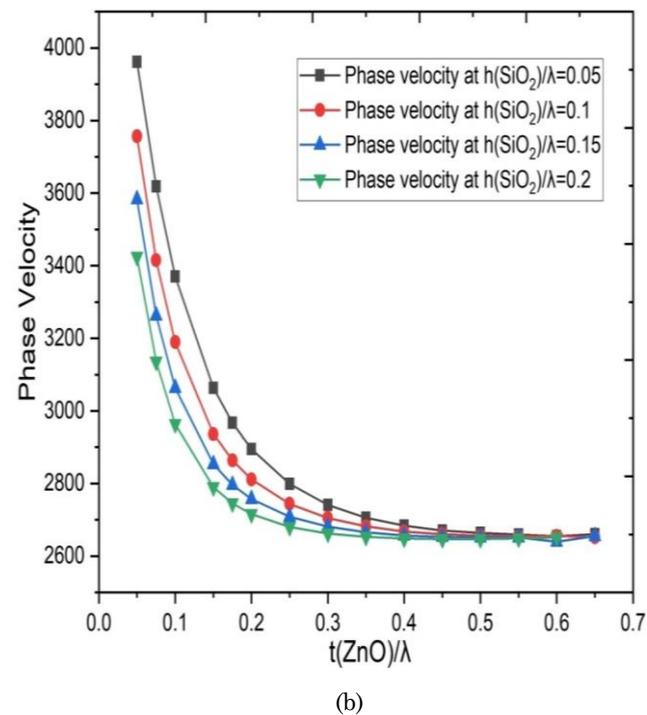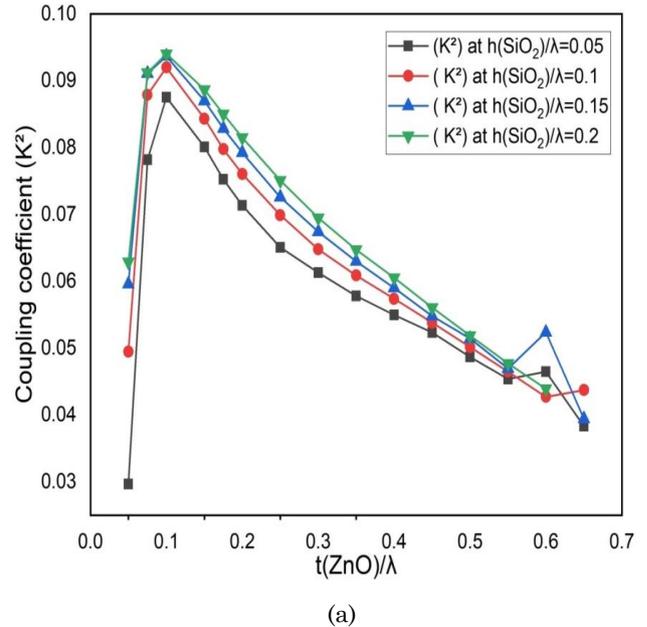
Fig. 3 – Simulated result of a) Electromechanical Coupling Coefficient (K^2) and b), phase velocity of Rayleigh mode generated in ZnO/(IDT)/ZnO/SiO₂/Si structure as function of normalized thickness of ZnO for different normalized thicknesses of SiO₂, respectively
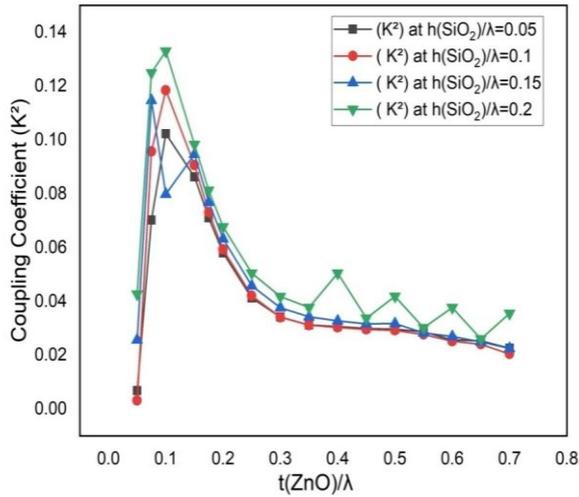
a)
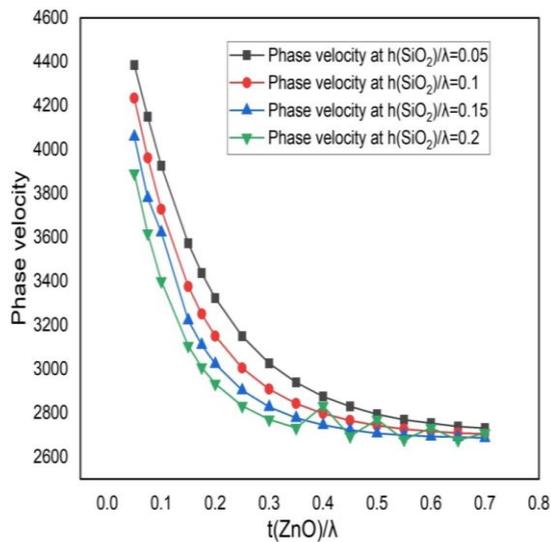
b)

Fig. 4 – Simulated result of a) Electromechanical Coupling Coefficient (K^2) and b) phase velocity of Rayleigh mode generated in ZnO/(IDT)/SiO$_2$/Si structure as a function of the normalized thickness of ZnO for different normalized thicnesses of SiO$_2$, respectively

Table 3 – Coupling coefficient (K2) and phase velocity of (IDT)/ZnO/SiO$_2$/Si, ZnO/(IDT)/ZnO/SiO$_2$/Si, and ZnO/(IDT)/SiO$_2$/Si structure with $(t_{(ZnO)}/\lambda) = 0.1$ and $(t_{(SiO2)}/\lambda) = 0.1$ value

Structure	Coupling Coefficient (K^2)	Phase velocity (m/s)
(IDT)/ZnO/SiO$_2$/Si	0.0094	3554
ZnO/(IDT)/ZnO/SiO$_2$/Si	0.091	3414
ZnO/(IDT)/SiO$_2$/Si	0.1184	4234

4. CONCLUSION

To improve the performance of CMOS compatible SAW device, we propose a three multilayer structures: (IDT)/ZnO/SiO$_2$/Si, ZnO/(IDT)/ZnO/SiO$_2$/Si, and ZnO/(IDT)/SiO$_2$/Si. The effect of the thicknesses of ZnO and SiO$_2$ thin films on three multilayer structures is numerically investigated using a 2D-finite element model for Rayleigh mode. The phase velocity of SAW generated in the three structures is strongly dependent on ZnO thickness and is inversely changes with the ZnO thickness. It is found that the optimized ZnO/(IDT)/SiO$_2$/Si multilayer structure exhibits the highest electromechanical coupling coefficient of 0.133 and high phase velocity of 4388 m/s at the normalized thickness $(t_{(ZnO)}/\lambda) = 0.1$ and $(t_{(SiO2)}/\lambda) = 0.2$. Also, we pointed that, with the introduction of SiO$_2$ layer can significantly improve the coupling coefficient (K^2) of structure. The results of simulations show that the by using an ZnO/(IDT)/SiO$_2$/Si multilayer structure, potential to integrated with CMOS compatibility, a high coupling coefficient and phase velocity achieved, which is impossible by employing the single bulk material and traditional device structure. From the result, we can conclude that the optimized ZnO/(IDT)/SiO$_2$/Si structure is promising for the realization of good-performance SAW filters at 915 MHz ISM band frequency.

AKNOWLEDGEMENTS

REFERENCES

1. H. Zhang, H. Wang, *Micromachines* **12** No 11, 1286 (2021).
2. J. Shen, et al., *IEEE Access* **8**, 123262 (2020).
3. D. Morgan, *Surface Acoustic Wave Filters, 2nd ed*. (Elsevier Ltd., UK: 2007).
4. A. Tezuka, H. Kuwae, K. Yamada, S. Shoji, S. Kakio, J. Mizuno, *Trans. Jpn. Inst. Electron. Packag.* **13**, E19-009 (2020).
5. C. Fu, et al., *Surf. Coat. Technol.* **363**, 330 (2019).
6. Y.Q. Fu, et al., *Prog. Mater. Sci.* **89**, 31 (2017).
7. M.B. Assouar, O. Elmazria, P. Kirsch, P. Alnot, V. Mortet, C. Tiusan, *J. Appl. Phys.* **101** No 11, (2007), doi: 10.1063/1.2739218.
8. P. Dutheil, J.C. Orlianges, A. Crunteanu, A. Catherinot, C. Champeaux, *phys. status solidi* **212** No 4, 817 (2015).
9. X.Y. Du, et al., *J. Phys. Conf. Ser.* **76**, 012035 (2007).
10. C. Sudhir, V.S. Atul, *Key Eng. Mater.* **500**, 84 (2012).
11. S.S. Shinde, K.Y. Rajpure, *J. Alloy. Compd.* **522**, 118

(2012).
12. G. Kaur, A. Mitra, K.L. Yadav, *Prog. Nat. Sci. Mater. Int.* **25** No 1, 12 (2015).
13. H.W. Kim, K.S. Kim, C. Lee, *J. Mater. Sci. Lett.* **22** No 15, 1117 (2003).
14. T. Saeed, P. O'Brien, *Thin Solid Films* **271** No 1-2, 35 (1995).
15. J.H. Visser, et al., *Ultrason. Symp. Proc.* **1**, 195 (1989).
16. S. Wu, R. Ro, Z.X. Lin, *Appl. Phys. Lett.* **94** No 3, 1 (2009).
17. S. Krishnamoorthy, A.A. Iliadis, *Solid. State. Electron.* **50** No 6, 1113 (2006).
18. S.J. Ippolito, K. Kalantar-Zadeh, W. Wlodarski, G.I. Matthews, *Proc. IEEE Sensors* **2** No 1, 539 (2003).
19. R. Su, et al., *ACS Appl. Mater. Interfaces* **12** No 37, 42378 (2020).
20. Y. Q. Fu, et al., *Sensor. Actuat. B* **143** No 2, 606 (2010).
21. S.L. Jiabao Yi, *Functional Materials and Electronics, 1 st*

Ed. (2018).

22. A. Hachigo, D.C. Malocha, *IEEE Trans. Ultrason. Ferroelectr. Freq. Control* **45** No 3, 660 (1998).

23. R. Li, et al., *ECS J. Solid State Sci. Technol.* **6** No 11, S3119 (2017).

24. M. Hanif, V. Jeoti, M.Z. Aslam, *J. Phys. Conf. Ser.* **1529** No 5, 052039 (2020).

25. G.S. Chung, D.T. Phan, *J. Korean Phys. Soc.* **57** No 3, 446 (2010).

26. M. Z. Aslam, V. Jeoti, S. Karuppanan, A.F. Malik, A. Iqbal, *Sensors* **18** No 6, 1687 (2018).